MOLECULAR AND CELLULAR BIOLOGY, Mar. 2011, p. 1041–1053 Vol. 31, No. 5
0270-7306/11/$12.00 doi:10.1128/MCB.01448-10

The ARID Family Transcription Factor Bright Is Required for both Hematopoietic Stem Cell and B Lineage Development▽

Carol F. Webb,[1]† James Bryant,[2]† Melissa Popowski,[2] Laura Allred,[2] Dongkoon Kim,[2] June Harriss,[2] Christian Schmidt,[2] Cathrine A. Miner,[1] Kira Rose,[1] Hwei-Ling Cheng,[3] Courtney Griffin,[4] and Philip W. Tucker[2]*

Immunobiology and Cancer Research Program[1] and Cardiovascular Biology Research Program,[4] Oklahoma Medical Research Foundation, Oklahoma City, Oklahoma 73126; Department of Molecular Genetics and Microbiology, Institute for Cellular and Molecular Biology, University of Texas at Austin, Austin, Texas 78712[2]; and Howard Hughes Medical Institute and Children's Hospital, Harvard Medical School, Boston, Massachusetts 02115[3]

Received 27 September 2010/Returned for modification 20 November 2010/Accepted 21 December 2010

***Bright*/*Arid3a* has been characterized both as an activator of immunoglobulin heavy-chain transcription and as a proto-oncogene. Although Bright expression is highly B lineage stage restricted in adult mice, its expression in the earliest identifiable hematopoietic stem cell (HSC) population suggests that Bright might have additional functions. We showed that >99% of *Bright*$^{-/-}$ embryos die at midgestation from failed hematopoiesis. *Bright*$^{-/-}$ embryonic day 12.5 (E12.5) fetal livers showed an increase in the expression of immature markers. Colony-forming assays indicated that the hematopoietic potential of *Bright*$^{-/-}$ mice is markedly reduced. Rare survivors of lethality, which were not compensated by the closely related paralogue Bright-derived protein (Bdp)/Arid3b, suffered HSC deficits in their bone marrow as well as B lineage-intrinsic developmental and functional deficiencies in their peripheries. These include a reduction in a natural antibody, B-1 responses to phosphocholine, and selective T-dependent impairment of IgG1 class switching. Our results place *Bright*/*Arid3a* on a select list of transcriptional regulators required to program both HSC and lineage-specific differentiation.**

The formation and maintenance of blood throughout fetal and adult life rely on the self-renewal of hematopoietic stem cells (HSCs). Rare HSCs arise in the embryonic yolk sac and aorta-gonad mesonephros AGM, seed the fetal liver, and then circulate in the bone marrow of adult mammals. Fetal and adult HSC progenitors become progressively dedicated to differentiation into erythrocytes, myeloid cells, and lymphocytes. Transcription factors critical for the specification and formation of HSCs cover a wide range of DNA binding protein families. An emerging theme is that many of these same regulators are required later for the differentiation of individual blood lineages, which explains why a number of HSC transcription factors were discovered and originally characterized because of their deregulation in hematopoietic malignancies.

Bright/Arid3a/Dril1 is the founder of the *A*T-*r*ich *i*nteraction *d*omain (ARID) superfamily of DNA binding proteins (18, 60). Bright, in a complex with Bruton's tyrosine kinase (Btk) and TFII-I, binds to specific AT-rich motifs within the nuclear-matrix attachment regions (MARs) of the immunoglobulin heavy-chain (IgH) intronic enhancer (Eμ) and selected IgH promoters to activate IgH transcription (18, 25, 30, 43, 44, 55, 57, 58). B cell-specific, transgenic overexpression of Bright leads to partial blocks at both the late-pre-B and T1 immature stages, skewed marginal-zone (MZ) B cell development, increased natural IgM antibody production, and intrinsic autoimmunity (49). Transgenic dominant negative (DN) inhibition of Bright DNA binding results in reduced levels of IgM in serum and functional perturbation of IgM secretion by B-1 cells (39, 48). A small pool of Bright cycles from the nucleus into plasma membrane lipid rafts, where it associates with Btk to dampen antigen receptor signaling (48).

While highly B lineage restricted in adult mice, Bright is expressed more broadly during embryonic development and is detectable in the earliest lymphoid progenitors (58). Ectopic overexpression of Bright in mouse embryonic fibroblasts (MEFs) overcomes natural or *rasV*^{12}-mediated senescence to promote cell cycle entry and *in vivo* transformation (42). Overexpression in the most highly aggressive subset of human diffuse large-B cell lymphomas (AID-DLBCL) has further implicated *Bright* as a proto-oncogene (38). The structure of the ARID DNA binding domain of Bright was solved (31) as part of the Human Cancer Protein Interaction Network (HCPIN) human cancer biology theme project (21), whose goal is to provide a three-dimensional (3D) structure database of human cancer-associated proteins.

These data forecasted functions for Bright beyond its established role as a regulator of IgH transcription. Through generation and analyses of null mice, we demonstrated that Bright/Arid3a can be added to the select list of DNA binding factors required for both HSC and lineage-specific differentiation.

MATERIALS AND METHODS

Construction and screening of a *Bright*/*Arid3a* null allele. Targeting arms devoid of repetitive sequences and as long as possible were identified within noncoding 5′- and 3′-flanking regions of the genomic *Bright* locus, allowing construction of a null mutation. A cloning strategy was optimized to ensure against spurious expression of the positive selectable marker via cryptic promoter sites within the targeting arms or recombined *Bright* locus. The 5′-targeting arm consisted of a 1.4-kb SmaI fragment cloned into pBluescript to introduce a

* Corresponding author. Mailing address: Department of Molecular Genetics and Microbiology, University of Texas at Austin, 1 University Station A5000, Austin, TX 78712. Phone: (512) 475-7705. Fax: (512) 475-7707. E-mail: philtucker@mail.utexas.edu.
† These authors contributed equally to this study.
▽ Published ahead of print on 3 January 2011.

multiple-cloning site to aid engineering of the construct. Similarly, the 3′ arm, a 3.4-kb BamHI fragment, was first cloned into pBluescript. These arms were introduced into a targeting vector, pPNT, containing the neomycin resistance (*Neo*^{r}; positive selection) and diphtheria toxin (*DT-A*; negative selection) genes. The incompatible ends between the *DT-A* marker (XhoI) and the pBluescript-generated EcoRI site of the 5′ arm were ligated after the ends were blunted. The 3.4-kb 3′ arm was excised from pBluescript as a XhoI/NotI fragment and inserted into the equivalent sites of pPNT.

SM1-129SVJ mouse embryonic stem (ES) cells were electroporated with the targeting vector, and clones that survived G418 selection were identified by Southern blotting of genomic DNA. To screen for homologous recombination of the 5′ arm, DNA from each clone was digested with DraI, fractionated by electrophoresis through 0.8% agarose gels, transferred to Nitran$^+$ membranes (Amersham), and hybridized with a 700-bp PstI genomic fragment 5′ of the 5′ arm. Wild-type (WT) ES cells exhibit a 9.0-kb DraI fragment, while *Bright*$^{+/-}$ ES cells produce the 9.0-kb (WT) DraI fragment and a 3.5-kb (mutant) fragment. For homologous recombination of the 3′ arm, DNA was digested with BglII and probed with an internal 0.4-kb AccI fragment. This process results in a 5.2-kb WT band, while the insertion of *Neo*^{r} during recombination results in a larger 6.4-kb band for *Bright*$^{+/-}$ cells. Correct gene targeting deletes the 8 Bright exons and introns (22.2 kb), leaving the *Neo*^{r} gene.

A correctly targeted clone was injected into embryonic day 3.5 (E3.5) C57BL/6 blastocysts, and the resulting chimeric males were mated to wild-type C57BL/6 females for germ line transmission of the altered allele. Because *Bright*$^{-/-}$ mice were embryonic lethal at E12.5, the strain was maintained by heterozygous breeding. For the studies reported here, *Bright*$^{+/-}$ mice were backcrossed with C57BL/6 mice for at least four generations. Genotyping of WT and disrupted *Bright* alleles was performed by PCR. The WT allele was identified by the production of a 200-bp PCR product with the *Bright*-specific primer pair 5′-TGAGTTCCCAAGGTCTGTGTGTTC-3′ and 5′-GGATCTCGTACCGTAAATGGCAGT-3′ . The *Bright* null allele was identified by the production of a 408-bp PCR product with Bright-specific (5′-GGAGTCTGCAGGTGCTTGAA-3′) and *Neo*^{r} cassette (5′-GATCAGCAGCCTCTGTTCCA-3′) primers. The samples were heated to 94°C for 2 min (WT) or 5 min (knockout [KO]) and subjected to amplification for 35 cycles of 0.5 min at 94°C, 0.5 min at 58°C (WT) or 62°C (KO), and 0.5 min at 72°C and, after the last cycle, an extension at 72°C for 7 min.

Construction and confirmation of *Bdp*/*Arid3b* null mice. A Bright-derived protein (Bdp) gene-trapped 129Sv ES cell line, RRJ028 (BayGenomics), was constructed via integration of a retroviral reporter (51) into intron 3/4. pGT1TMpfs contains a splice acceptor sequence upstream of a reporter gene, β*geo* (a fusion of β-galactosidase and *Neo*^{r}). Splicing of the pre-mRNA results in a non-DNA binding fusion protein that expresses the β*geo* marker and terminates within the second ARID-encoding exon. The exact fusion site was determined by DNA sequencing using *geo* primer 5′-GACAGTATCGGCCTCAGGAAGATCG-3′ and confirmed by PCR using a *Bdp*-exon 3 primer, 5′-TCGACAATCTGTAAGGCGACT-3′, with the vector-derived primer 5′-CACTCCAACCTCCGCAAACTC-3′. Blastocyst injections, chimera analysis, and backcrossing were performed as described above for Bright. Verification of germ line transmission was performed on tail DNA digested with NcoI using two external 5′ fragments as Southern probes, producing a *Bdp* WT band of 4 kb and a disrupted *Bdp* band of 9 kb.

Reverse transcription (RT)-PCR analyses. Total RNA was isolated from embryonic and adult tissues or from splenic B cells purified by passage over anti-CD43 magnetic beads (Miltenyi Biotec), with or without 24-h lipopolysaccharide (LPS) stimulation, using an RNeasy kit (Qiagen). Oligo(dT)- and random-hexamer-primed cDNA was then prepared according to the Superscript II protocol (Gibco/BRL). Levels of Bright were assessed using primers that amplify 390-nucleotide (nt)-spanning *Bright* exons 3 and 4 (forward primer, 5′-GCGGACCCCAAGAGGAAAGAGTT-3′; reverse primer, 5′-CTGGGTGAGTAGGCAAAGAGTGAGC-3′), Bdp exons 5 and 6 (412 bp; forward primer, 5′-TGGCTGTGTCAGGGACTTTGG-3′; reverse primer, 5′-TCTCGAATTCCCTTCTGGTAGTTCTGTTCT-3′), β-major globin (590 bp; forward primer, 5′-CGTTTGCTTCTGATTCTGTTG-3′; reverse primer, 5′-CTAGATGCCCAAAGGTCTTC-3′), β-minor globin (411 bp; forward primer, 5′-AAAGGTGAACCCCGATGAAG-3′; reverse primer, 5′-TGTGCATAGACAATAGCAGA-3′), E-Y globin (535 bp; forward primer, 5′-TGACACTCCTGTGATCACCA-3′; reverse primer, 5′-AAAGGAGGCATAGCGGACAC-3′), B-H1 globin (498 bp; forward primer, 5′-TCTCCAAGCTTCTATACCTC-3′; reverse primer, 5′-CATGGGATTGCCAGTGTACT-3′), and β-actin (1,038 bp; forward primer, 5′-CAAGGTGTGATGGTGGGAAT-3′; reverse primer, 5′-CAAGGTGTGATGGTGGGAAT-3′).

Levels of mature (VDJ-Cμ) transcripts were measured as previously described (2, 14), coupling a Cμ1-derived reverse primer (5′-ATGCAGATCTCTGTTTTTGCCTCC-3′) with forward primers specific for V_HJ558 (5′-CGAGCTCTCCARCACAGCCTWCATGCARCTCARC-3′), V_H783 (5′-CGGTACCAAGAASAMCCTGTWCCTGCAAATGASC-3′), V_H3609 (5′-KCYYTGAAGAGCCRRCTCACAATCTCC-3′), and V_HS107 (5′-CTTCTGGGTTCACCTAGA-3′).

Germ line-initiated (I) heavy-chain transcripts were measured as previously described (32), using the following primer pairs: $I_{\gamma 3}$ (forward primer, 5′-CAAGTGGATCTGAACACA-3′; reverse primer, 5′-GGCTCCATAGTTCCATT-3′), $I_{\gamma 1}$ (forward primer, 5′-CAGCCTGGTGTCAACTAG-3′; reverse primer, 5′-GCAAGGGATCCAGAGTTCCAG), $I_{\gamma 2a}$ (forward primer, 5′-CTTACAGACAAGCTGTGACC-3′; reverse primer, 5′-AACGTTGCAGGTGACGGTCTC-3′), $I_{\gamma 2b}$ (forward primer, 5′-CCTGACACCCAAGGTCACG-3′; reverse primer, 5′-CGACCAGGCAAGTGAGACTG-3′), and I_ε (forward primer, 5′-GACGGGCCACACCATCC-3′; reverse primer, 5′-CGGAGGTGGCATTGGAGG-3′). Samples were electrophoresed through 1.0% agarose gels, and the relative intensities of the PCR products were quantified using LumiAnalyst 3.0 software (Roche, Indianapolis, IN).

Histological procedures. Mice were euthanized under the guidelines of the IACUC and our institutions. Adult tissues and embryos, collected at the number of days postconception indicated in the figures, were fixed in 4% paraformaldehyde for 24 to 48 h, dehydrated through a series of ethanol solutions, and then embedded in paraffin. Hematoxylin and eosin (H&E) staining, *in situ* hybridization, immunohistochemistry, and terminal deoxynucleotidyltransferase-mediated dUTP-biotin nick end labeling (TUNEL) were performed as previously described (17, 54). The Bright *in situ* RNA probe and hybridization conditions were previously described (18, 30). Anti-Bright antibody (affinity purified, rabbit polyclonal; 1:2,000) was prepared as previously described (18). Anti-CD31 antibody (mouse monoclonal; 1:100) was purchased from Santa Cruz Biotechnologies and Ki67 antibody (mouse monoclonal; 1:400) from Cell Signaling Technologies. To quantify cells positive for Bright, TUNEL, Ki67, and globin, 3 fields of view for 3 embryos of each genotype and age were viewed at a magnification of ×400 and counted.

Cell separations and flow cytometry. Bone marrow or E12.5 fetal liver cells were enriched for lineage-negative cells by incubation with antibodies (BD Pharmingen) to lineage markers, anti-Gr-1 (Ly-6G, RB6-8C5), and anti-CD11b/Mac-1 (M1/70) for myeloid cells, anti-CD19 (1D3) and anti-CD45R/B220 (RA3-6B2) for B lineage cells, CD8α (53-6.7) and CD8β (53-5.8) for T cells, and anti-Ter-119 for erythroid cells, followed by negative selection using the MACS cell separation system (Miltenyi Biotec, Auburn, CA). The same antibodies without CD11b/Mac-1 were used for lineage depletion of fetal liver. Unfractionated and partially lineage-depleted bone marrow and fetal liver cells were stained with fluorescein isothiocyanate (FITC)-antilineage monoclonal antibodies (MAbs) Gr-1, Mac-1 (adult only), Ter-119, and CD45R as well as anti-stem cell MAbs phycoerythrin (PE)-Sca-1 (Ly6A/E, E13-161.7) and allophycoerythrin (APC)-c-kit (2B8). MAbs were purchased from BD Pharmingen.

Cell surface phenotypes of lymphocyte populations in adult thymus, spleen (harvested as single-cell suspensions in RPMI medium with 7% fetal calf serum [FCS]), and peritoneal cavity (obtained by lavage with phosphate-buffered saline [PBS]–3% FCS) utilized the additional BD Pharmingen MAbs: FITC-CD21 (7G6) and CD4 (RM4-4), PE-CD8 (53-6.7), CD3 (145-2C11), CD43, CD40 (1C10), CD69 (Hi.2F3), APC-CD45R/B220 (RA3-6B2), and PerCP-CD45R/B220 (RA3-6B2). FITC-IgM, PE-IgD, goat anti-mouse IgM, appropriate isotype controls, and streptavidin-conjugated APC were obtained from BD or Southern-Biotech (Birmingham, AL). Adult splenic bone marrow and thymic subpopulations were identified as described in Shankar et al. (49). Fetal liver and bone marrow hematopoietic populations were defined and measured according to Chen et al. (9).

Cells (~1.5×10^6) were fixed in 0.2% paraformaldehyde overnight and stained as previously described (58). Flow cytometry was performed on a FACSCalibur instrument (Becton Dickinson, Mountain View, CA) or on an LSR11 flow cytometer (BD Biosciences, San Jose, CA). Cell-sorting experiments were performed on a FACSAria cell sorter (Becton Dickinson, Franklin Lakes, NJ). The data were analyzed with either FlowJo (Tree Star, San Carlos, CA) or CellQuest Pro software (BD Biosciences). Gates set in the lower panel of Fig. 3C are specified as low (lo) or high (hi) relative to mean fluorescence intensity.

Adoptive transfer. Bone marrow (~5×10^6 cells) from *Bright*$^{-/-}$ and *Bright*$^{+/-}$ adult mice (4 to 6 weeks old) was injected intravenously into sublethally (500-rad) irradiated C57BL/6 recipients. Four weeks later, bone marrow cells, splenocytes, and thymocytes were harvested from these mice and chimerism was confirmed by flow cytometry.

Rag2$^{-/-}$ blastocyst complementation. To obtain *Bright*$^{-/-}$ ES lines, blastocysts were flushed out of the horns of 3.5-days-pregnant *Bright*$^{+/-}$ females that had been mated with *Bright*$^{+/-}$ males (20). Blastocysts were transferred onto STO feeder layers in ES media (Dulbecco's modified Eagle medium [DMEM] supplemented with 20% fetal bovine serum [FBS], penicillin/streptomycin,

nucleosides, nonessential amino acids, and β-mercaptoethanol) and cultured at 37°C in 5% CO_2 in humidified air for 6 to 7 days without media changes. The inner cell masses were identified, treated with trypsin, disrupted, and then transferred individually and subcultured in 24-well STO feeder plates. Four days later, single-cell clones of compact ES colonies were passaged onto 6-well plates and then split after 2 to 3 generations for confirmation of the *Bright* null genotype by PCR.

Rag2$^{-/-}$ mice were maintained in a pathogen-free facility, and 4- to 8-week-old females were used as blastocyst donors. *Rag2*$^{-/-}$ blastocysts were recovered from the uteruses of 3.5-days-postcoitum pregnant females and were injected as described previously (8) with 3 *Bright*$^{-/-}$ and 2 *Bright*$^{+/-}$ clones. Injected embryos were then transferred into the uteruses of synchronized pseudopregnant foster mothers. Chimeric offspring were identified by agouti coat color and PCR analysis of tail DNA for the *Bright* null allele. Reconstituted lymphocytes were verified by fluorescence-activated cell sorter (FACS) analysis of peripheral blood at 4 to 6 weeks.

Cell culture and *in vitro*-stimulation assays. Mouse hematopoietic progenitors from fetal liver were assessed using a methylcellulose colony assay. Assays were initiated with 300,000 cells per dish using MethoCult GF M3434 (StemCell Technologies) according to the manufacturer's directions. Cultures were incubated for a total of 14 days but were checked on day 7 for erythroid burst-forming units (BFU-E) and on day 12 for CFU granulocyte macrophages (CFU-GM) and CFU granulocyte erythrocyte monocyte macrophages (CFU-GEMM). Colonies were analyzed visually and were counted using a Nikon TS100 inverted microscope.

Splenic B cells were T cell depleted using anti-Thy-1 and guinea pig complement and isolated by centrifugation through a Ficoll gradient or enriched by exclusion over CD43-coupled magnetic beads (Miltenyi Biotec) as previously described (48, 59). Cells were plated at ~5×10^6 cells/ml in RPMI medium (supplemented with 10% heat-inactivated fetal calf serum, 100 U/ml penicillin, 100 μg/ml streptomycin, 5×10^{-5} M β-mercaptoethanol, and 1 mM sodium pyruvate) alone or with 20 μg/ml LPS (*Escherichia coli* 0111:1B4; Sigma, St. Louis, MO) or anti-IgM (50 μg/ml) or anti-CD40 (20 μg/ml) with interleukin-4 (IL-4; 50 ng/ml). After 72 h, cells and supernatants were harvested for flow cytometry, enzyme-linked immunosorbent assays (ELISAs), or mature and germ line isotype analyses. In some cases, wells were pulsed with 1 μCi of ^{3}H-thymidine for 6 h and harvested, and the incorporation of ^{3}H was measured.

Immunizations. Mice (at least 6 weeks old) were immunized intravenously (i.v.) with trinitrophenol (TNP)-keyhole limpet hemocyanin (KLH) (0.5 μg/ml) in Freund's complete adjuvant (Sigma, St. Louis, MO) as previously described (49). Mice were boosted on day 7 with the same dose of antigen. Sera were collected at days 0, 7, and 14 postimmunization. Mice were also immunized i.v. with ~1×10^8 heat-killed, pepsin-treated *Streptococcus pneumoniae* (strain RSA32) cells as previously described (6). Seven days later, sera were collected for ELISAs.

ELISAs. A Clonotyping system/AP kit (Southern Biotechnology Associates) was used, according to the manufacturer's directions, to test for serum isotypes and isotypes generated by *in vitro* stimulations. Standard curves were generated with isotypes of known concentrations, and Ig levels were quantified using Microsoft Excel software. Antigen-specific antibodies were detected using phosphocholine (PC)-, bovine serum albumin (BSA)-, or TNP-BSA-coated plates, as described previously (23, 58). Samples were assessed in triplicate at four or more dilutions, and samples were read with an MRX microtiter reader (Dynatech Laboratories).

RESULTS

The majority of conventional *Bright* knockout mice die at midgestation. A null allele of *Bright*/*Arid3a* was constructed and confirmed in 129Sv ES cells (Fig. 1A to C). Following germ line transmission into 129Sv or C57BL/6 mice, *Bright* heterozygotes had no apparent pathology (data not shown). Greater than 99% of *Bright*$^{-/-}$ mice generated from multiple chimeras were embryonic lethal in both backgrounds. Death occurred between E11.5 and E13.5 (data not shown). Both *Bright* null embryos still alive at E12.5 and rare adult survivors were significantly smaller than their littermate controls (Fig. 1D).

Death of *Bright*$^{-/-}$ embryos results from failed erythropoiesis. While *Bright* mRNA is expressed broadly during early (E5.5 to E8.5) embryogenesis (data not shown), Bright protein is most highly expressed in the fetal liver at E12.5 (Fig. 2A). Although there was no evidence of hemorrhage, subcutaneous edema, or pericardial effusion (Fig. 2 A,B), *Bright* null embryos and yolk sacs were strikingly pale at E12.5 (Fig. 2B). This pallor was not associated with any apparent defect in cardiac function (data not shown) nor with vascular development, as determined by comparable anti-CD31 immunostaining in control and mutant embryos (Fig. 2C). However, cellularity of the E12.5 mutant livers was dramatically reduced (Fig. 2D). We also noted a reduction in thickness of the myocardial compact zone in E12.5 *Bright* null embryos (Fig. 2A and data not shown). These features suggested a critical and hitherto unexpected function for Bright/ARID3a in hematopoiesis.

Primitive erythropoiesis and globin switching are normal in *Bright* knockout embryos. In order to determine whether the pallor of *Bright*$^{-/-}$ embryos is due to failed HSC formation or maintenance, we examined embryos at earlier developmental stages. The extraembryonic yolk sac is the initial site of hematopoiesis and produces primitive blood cells that circulate between the yolk sac and embryo by E8.25. Our analysis of E9.5 embryos and yolk sacs confirmed that there were comparable numbers of erythrocytes in control and mutant littermates (Fig. 2Ea to d). Moreover, *Bright*$^{-/-}$ erythrocytes did not undergo aberrant apoptosis at E9.5, as evidenced by a lack of TUNEL staining in mutant blood cells (Fig. 2Ee to g). Therefore, primitive erythrocyte formation and maintenance appear unaffected by the loss of *Bright*.

Lethality in *Bright* null embryos occurs during the time interval in which erythropoiesis shifts in location from the yolk sac to the fetal liver. Primitive erythrocytes produced in the yolk sac express both embryonic and adult globin genes, while definitive erythrocytes produced in the liver express only adult globins. We saw comparable levels of embryonic and adult globin expression in mutant and control erythrocytes at E12.5 (Fig. 2F), indicating that globin switching is unaffected by the loss of *Bright*.

Bright knockout impairs embryonic HSC differentiation. Because the *Bright*$^{-/-}$ fetal livers showed generally decreased cellularity, we reasoned that fetal liver-derived hematopoietic differentiation in *Bright* null embryos might be compromised. c-kit is a progenitor cell marker expressed on HSCs, BFU-E, and erythroid CFUs (CFU-E). c-kit$^+$ Ter119$^+$ cells mark proerythroblasts and basophilic erythroblasts, whereas Ter119 single-positive cells are fully differentiated. Flow cytometry indicated that the percentages of mature c-kit$^-$ Ter119$^+$ cells were significantly reduced in *Bright*$^{-/-}$ fetal livers (Fig. 3A). These data were supported by May-Grunwald Giemsa stains of E12.5 wild-type and Bright null fetal liver cells (Fig. 3B). Of a total of 1,000 cells counted, approximately equal numbers of nucleated cells and enucleated pink cells (which represent mature erythrocytes) were contained in wild-type livers, while approximately half the number of enucleated cells as nucleated cells were contained in knockout livers. These data suggest that a differentiation defect might account for the lower number of erythroid cells in the Bright null fetal livers.

Further analyses of *Bright*$^{-/-}$ fetal livers indicated that in addition to the numbers of erythrocyte progenitors, the total numbers of lineage-negative (lin$^-$) c-kit^{hi} Sca1$^+$ (LSK) cells were substantially reduced. Both lin$^-$ c-kit$^+$ Sca1$^-$ (myeloid-lineage progenitor; MLP) and lin$^-$ c-kit^{lo} Sca1$^+$ (common

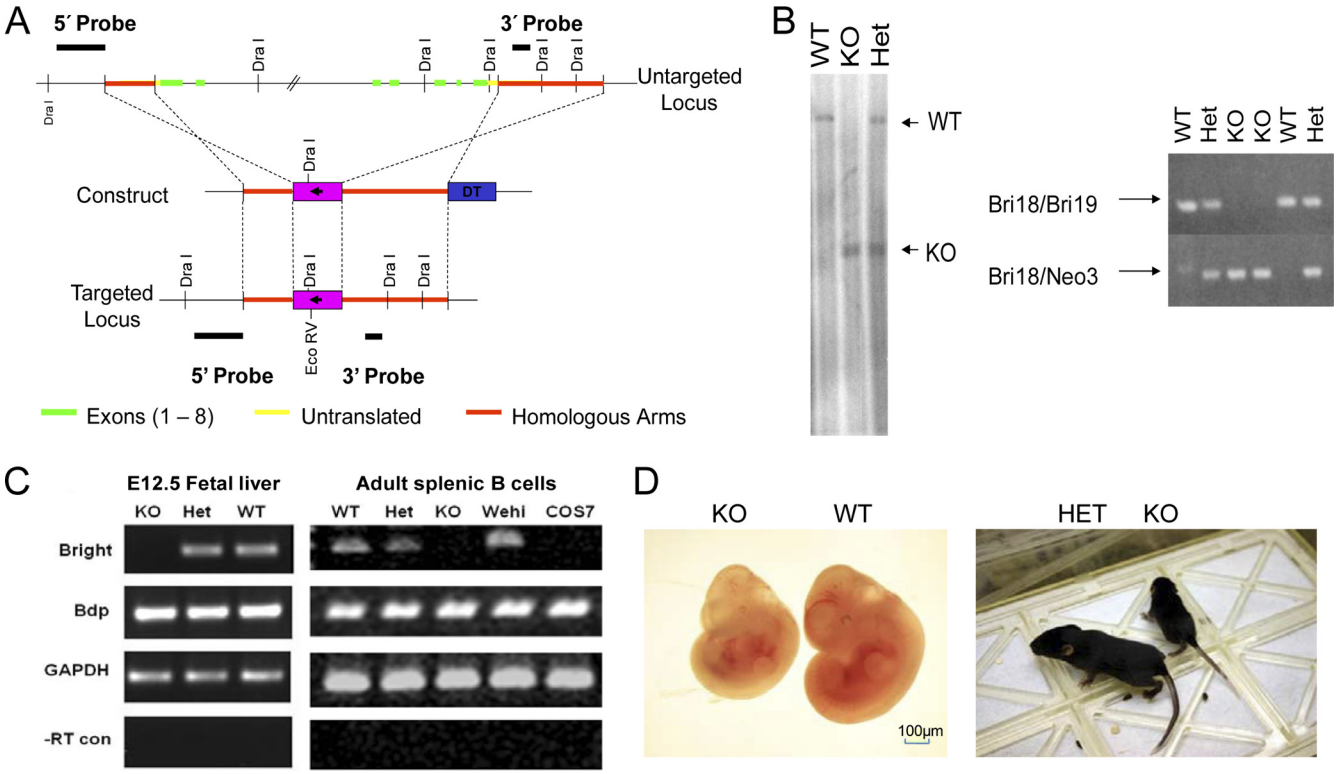

FIG. 1. Construction and confirmation of *Bright* null mice. (A) Schematic of the *Bright* locus and knockout strategy. The *Bright* transcription unit is composed of 8 exons spanning ~50 kb. Exon (untranslated, yellow; translated, green) regions are flanked by short (~1.3-kb) and long (~4.3-kb) arms of homology (red) in the targeting vector (middle panel). Neomycin (pgk-neo, pink) and diphtheria toxin (blue) cassettes are included for positive and negative selection, respectively. Also shown are the DraI restriction sites and locations of the probes used for Southern blot screening. (B) Left, Southern blot of tail DNA prepared from wild-type (WT), null (KO), and heterozygous (Het) littermates using the external 5′ probe shown in panel A. Right, PCR screen on tail DNA using either a primer pair that amplifies the WT (Bri18/Bri19) or a primer pair that amplifies the neomycin resistance cassette (Bri18/Neo3) inserted into the *Bright* locus following homologous recombination. (C) The knockout strategy results in a complete loss of *Bright* mRNA expression. RT-PCR employing primers spanning exons 3 and 4 was performed on cells in which the highest level of *Bright* expression is normally observed, E12.5 fetal liver (left panels) and adult splenic B cells stimulated with LPS (right panels), and on WEHI 231 B cells and COS-7 cells used as positive and negative controls, respectively. Note that expression of *Bright's* closest paralogue, *Bdp*/*Arid3b*, is not altered by *Bright* KO. (D) *Bright*$^{-/-}$ E12.5 embryos (left) and rare *Bright* null survivors (17 days, right) are significantly smaller than their WT and HET littermates.

lymphoid progenitor; CLP) subpopulations were also reduced ~2-fold, consistent with the generally smaller size of the fetal livers from the *Bright*$^{-/-}$ mice (Fig. 3C). However, colony-forming assays initiated with the same total numbers of wild-type and knockout cells revealed that the hematopoietic potential of knockout cells to yield B lymphocytes, erythromyeloid colonies, and BFU-E was reduced ~80% from that of normal controls (Fig. 3D), suggesting that Bright deficiency results in defective hematopoiesis in the fetal liver.

Bright is required for lymphopoiesis and conventional B cell differentiation in adults. The rare survivors (<1%) of *Bright*$^{-/-}$ lethality, although significantly smaller (Fig. 1D),

FIG. 2. Analysis of *Bright* null embryos. (A) *Bright* expression in E12.5 embryos is restricted primarily to the fetal liver (arrows). Sections from a *Bright* knockout embryo and a control littermate embryo were stained with anti-Bright antibody (top and bottom) or an isotype control (anti-IgG; middle). Red arrows indicate punctate areas of intense staining within the intestine. No morphological pathogenesis was observed elsewhere. Magnification: upper panel, ×25; lower panel, ×200. (B) *Bright*$^{-/-}$ embryos exhibit extreme pallor at E12.5. A *Bright* knockout embryo has significantly fewer circulating erythrocytes than its littermate control in both the yolk sac (left panel) and the embryo (right panel). (C) *Bright*$^{-/-}$ embryos show normal expression of the endothelial cell marker CD31, suggesting that vascular development is normal. Sections from E12.5 *Bright*$^{-/-}$ and control *Bright*$^{+/+}$ embryos were stained with hematoxylin (HE, left) and anti-CD31 (right). (D) E12.5 *Bright*$^{-/-}$ fetal livers are hypocellular. Whole E12.5 fetal livers from 33 wild-type (WT) and 25 *Bright* null (KO) embryos were isolated and placed in a single-cell suspension, and total cell numbers were counted. Student's *t* test shows significantly lower numbers of cells in the *Bright* null livers. (E) E9.5 *Bright*$^{-/-}$ erythrocytes are normal. Wild-type and *Bright*$^{-/-}$ littermate embryos (A and B) and yolk sacs (C and D) contain blood vessels with comparable numbers of circulating erythrocytes. Erythrocytes found in wild-type and *Bright*$^{-/-}$ embryonic vessels (E and F) and yolk sac vessels (G and H) are nonapoptotic, as evidenced by a lack of TUNEL staining (blue, DAPI; green, TUNEL). Blood vessels are outlined for identification. Scale bars, 100 μm. (F) The reduced number of Ter119^{+} null fetal liver reticulocytes at E12.5 contain levels of embryonic (εY and βH1) and fetal/adult (β^{maj} [B Major] and β^{min} [B Minor]) globins comparable to those of the controls. RT-PCR and cell fractionations were performed as detailed in Materials and Methods.

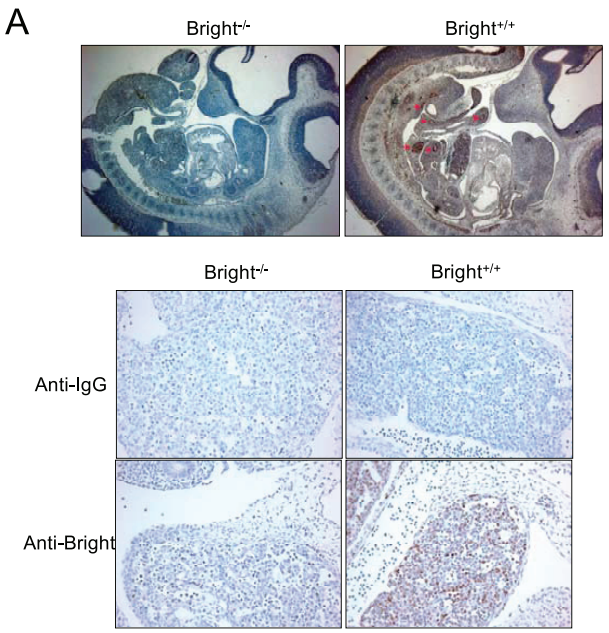
A
Bright-/-
Bright+/+
Bright-/-
Bright+/+
Anti-IgG
Anti-Bright

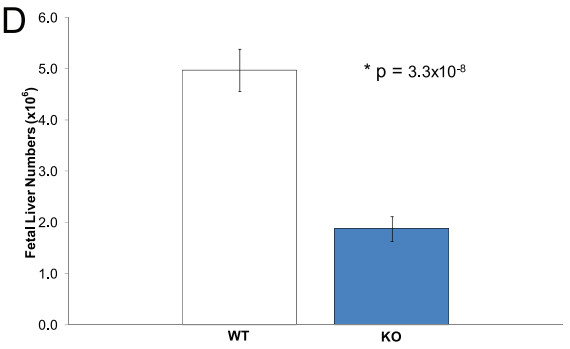
D
6.0
5.0
4.0
3.0
2.0
1.0
0.0
Fetal Liver Numbers (x10^6)
* p = 3.3x10^-8
WT
KO

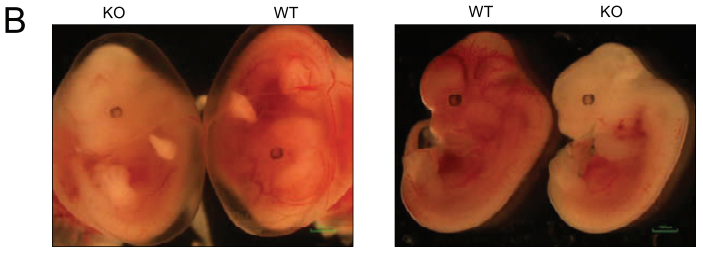
B
KO
WT
WT
KO

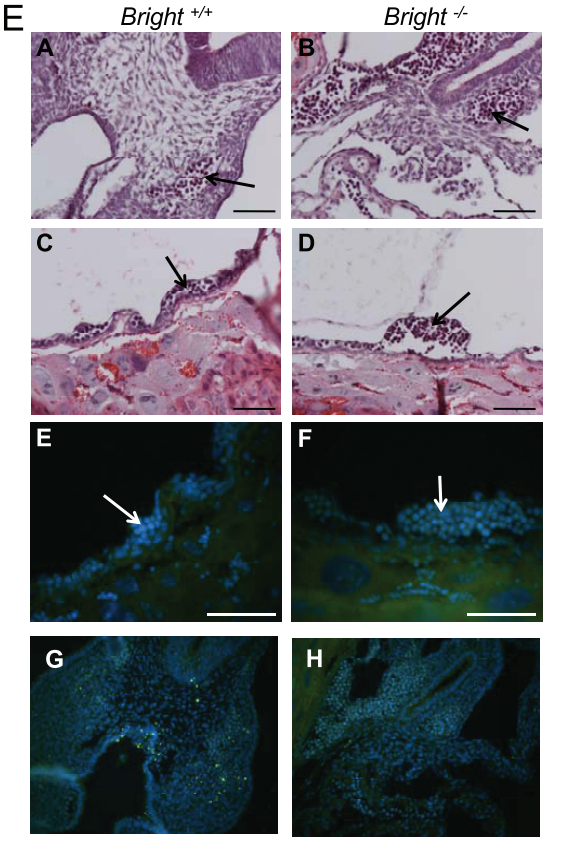
E
Bright +/+
Bright -/-
A
B
C
D
E
F
G
H

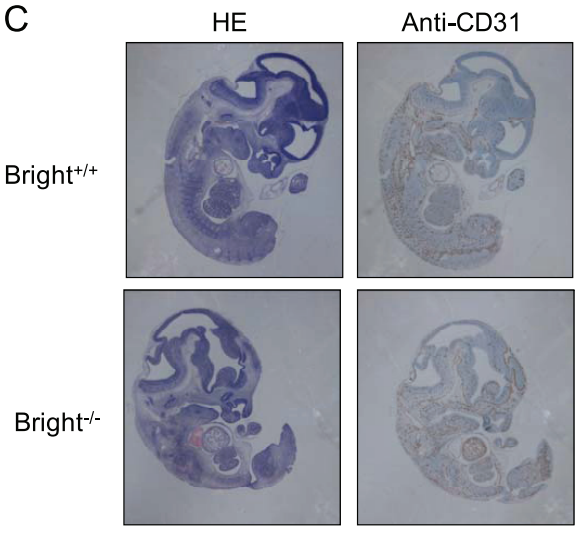
C
HE
Anti-CD31
Bright+/+
Bright-/-

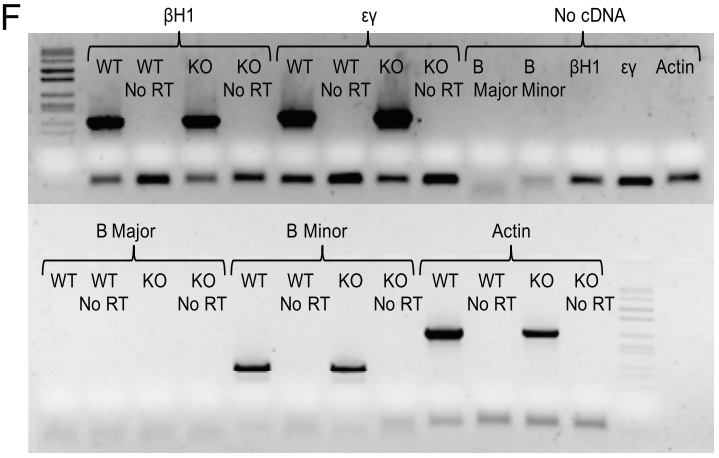
F
βH1
εγ
No cDNA
WT WT KO KO WT WT KO KO B B βH1 εγ Actin
No RT No RT No RT No RT Major Minor
B Major
B Minor
Actin
WT WT KO KO WT WT KO KO WT WT KO KO
No RT No RT No RT No RT No RT No RT No RT

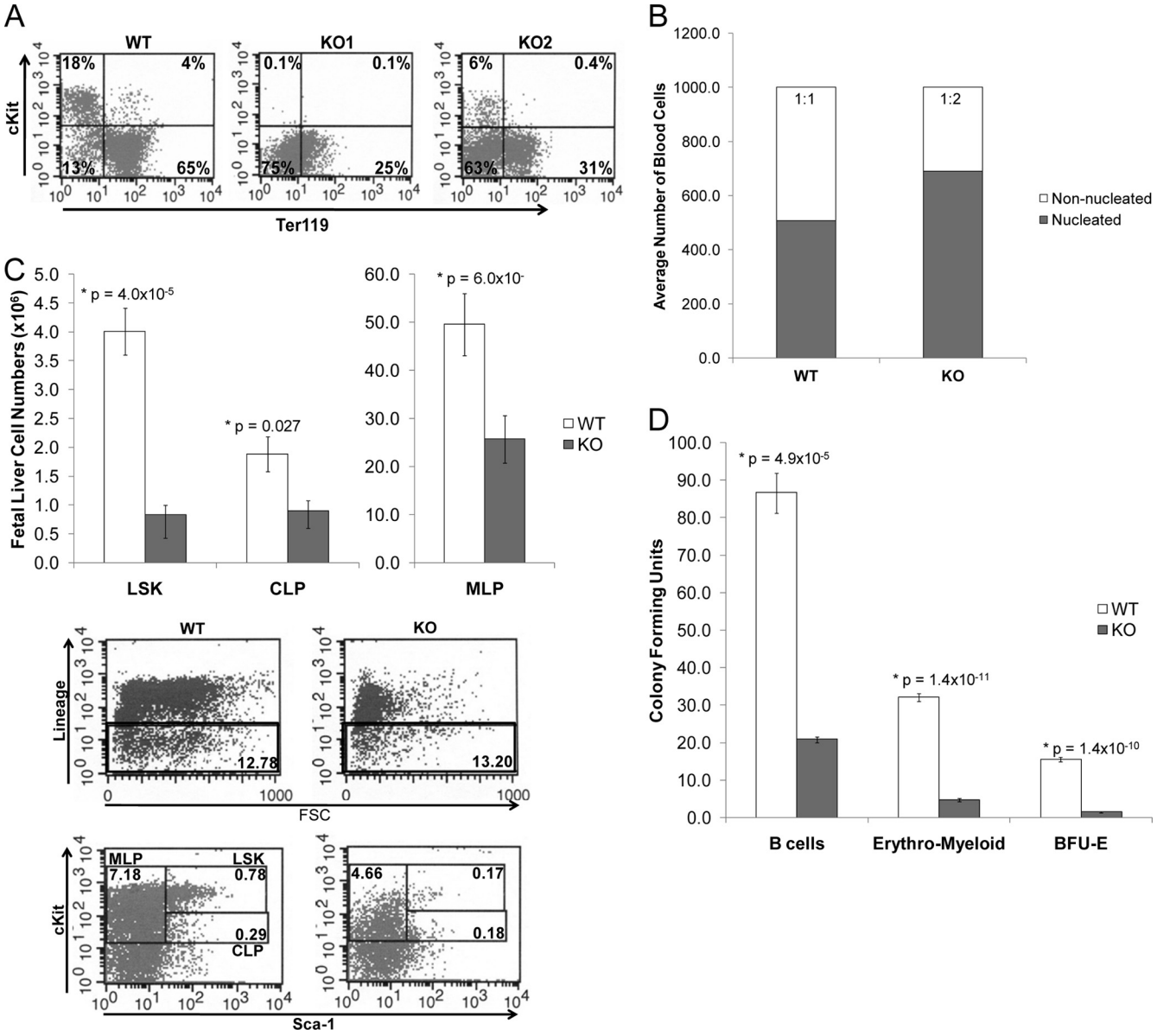

FIG. 3. *Bright* knockout impairs hematopoietic lineage differentiation. (A) Percentages of mature erythrocyte are decreased in *Bright* null fetal livers. E12.5 wild-type (WT) and *Bright* $^{-/-}$ (KO1 and KO2) fetal liver cells were stained with antibodies to c-kit and the mature marker Ter119 and analyzed by flow cytometry. (B) Comparison of May-Grunwald Giemsa stains of E12.5 *Bright*$^{-/-}$ and *Bright*$^{+/+}$ fetal livers showed fewer enucleated mature erythrocytes in the knockout livers. Ratios of total nucleated and enucleated (mature erythrocyte) cells were compared. (C) Total numbers of early lineage progenitors are decreased in E12.5 *Bright*$^{-/-}$ fetal livers compared to those in *Bright*$^{+/+}$ littermate controls. (Upper panel) Mean numbers (with standard errors) of lineage negative (Lin$^-$) c-kit^{hi} Sca1$^+$ (LSK), Lin$^-$ c-kit$^+$ Sca1$^-$ (myeloid lineage progenitor, MLP), and Lin$^-$ c-kit^{lo} Sca1$^+$ (common lymphoid progenitor, CLP) subpopulations from 21 knockout (KO) and 31 control mice. (Lower panel) Representative flow cytometry results and gates used for fetal liver progenitor data. (D) *Bright*$^{-/-}$ (KO) fetal liver cells are impaired in their ability to generate B, erythromyeloid, and BFU-E colonies in methylcellulose cultures compared to that of *Bright*$^{+/+}$ controls (WT). Data were obtained from duplicate samples from 3 to 5 mice. Standard error bars are shown.

showed no gross defects in organogenesis (data not shown). We observed a modest ($P = 0.10$) reduction in splenic cellularity, but this decrease did not result from differences in proliferation or apoptosis (data not shown). Erythrocyte numbers in peripheral blood showed no consistent differences among seven 3- to 9-month-old *Bright*$^{-/-}$ mice and six littermate controls (data not shown).

We reasoned that the erythropoietic compensation in these rare Bright null survivors might be provided by its closely related paralogue, Bdp/Arid3b (60). Bright and Bdp are highly similar across their entire open reading frames, share identical DNA binding properties, form immunoprecipitable protein complexes, and transactivate the IgH locus through the same *cis*-acting MARs (25, 40). However, upregulation of Bdp was

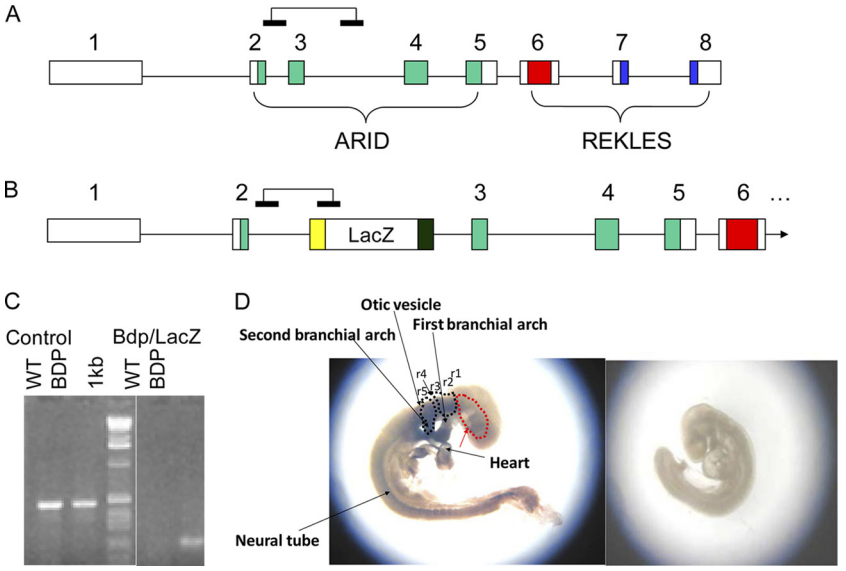

FIG. 4. $Bdp^{-/-}$ embryos die of neural crest defects and share no phenotype with $Bright^{-/-}$ embryos. (A) Map of wild-type *Bdp.* Exons are indicated by boxes, with ARID DNA binding domains (green) and REKLES self-association, nuclear import, and nuclear export domains (red and blue). (B) *Bdp* with the *LacZ* retroviral insertion (5′ long terminal repeat [LTR], yellow; 3′ LTR, black). Connected horizontal bars above each map indicate positions of primers used to distinguish germ line (A) and *LacZ*-retroviral integration (B) alleles by PCR. (C) Evidence of germ line transmission of the *LacZ* integration within *Bdp*. PCR was performed on tail DNA of first-generation founder mice as detailed in Materials and Methods. (D) Comparison of $Bdp^{+/+}$ (WT, right) and $Bdp^{-/-}$ (KO, left) embryos that survived to E9.5 (the majority die earlier). The KO embryos are developmentally delayed and show prominent levels of LacZ surrogate Bdp expression in neural crest cells of branchial arches and the neural tube. Dotted black lines indicate the general regions of rhombomeres 3 and 5 (r3 and r5) of the neural crest (note area between, where r4 should exist, but which is a neural crest-free region). A dotted red line surrounds the frontonasal prominence where a faint LacZ signal appears.

not observed in *Bright* knockout mice (Fig. 1C). Furthermore, *Bdp* null embryos were lethal at a significantly earlier (E7.5 to E9.5) stage and did not phenocopy $Bright^{-/-}$ HSC defects (Fig. 4) (addressed further in the Discussion). This finding, along with the observation that adult $Bdp^{+/-}$ by $Bright^{+/-}$ compound heterozygotes showed no measureable phenotype, led us to conclude that paralogous redundancy could not account for the occasional survival.

While an unknown mechanism can apparently offset erythropoietic defects, such was not the case for lymphopoiesis. As anticipated from the results shown in Fig. 3, both total cell numbers and frequencies of LSK (c-kit^{hi} Sca1^{+}), MLP (c-kit^{+} Sca1^{-}), and CLP (c-kit^{lo} Sca1^{+} IL7R^{+}) cells were significantly reduced in the bone marrow of 1- to 4-month-old *Bright* null mice (Fig. 5A). However, further differentiation was perturbed only in B lineages (Fig. 5B); T cell numbers and subset frequencies in these *Bright* null adults were comparable to those of wild-type controls (Fig. 5B). Strong blocks to conventional (B-2) pro- and pre-B development were observed in $Bright^{-/-}$ bone marrow. Peripheral $Bright^{-/-}$ B cell subsets (e.g., transitional and marginal zone B cells [MZB]), in which Bright is most highly expressed in normal cells (39, 48), were also significantly reduced (Fig. 5B). We observed modest reduction in $Bright^{-/-}$ follicular (FO) and circulating B cell numbers, subpopulations in which Bright expression is normally low, suggesting that homeostatic effects result in compensation of FO B cell numbers in adult spleens (Fig. 5B).

B-1 cell generation and function is impaired in $Bright^{-/-}$ adults. In addition to conventional B-2 cells, which comprise the great majority of the peripheral subsets, bone marrow progenitors of B-1 cells (CD93^{+} lin$^{-/lo}$ CD19^{+} CD45R^{-}) were also significantly reduced (Fig. 5A). Accordingly, mature B-1 cells (particularly the B-1a subset), which are the predominant B cell population in the peritoneal cavity, were depleted (Fig. 6A).

The B-1a subset is a major producer of natural serum antibody (33, 34). We observed reduced numbers of circulating antibodies, particularly IgM and IgG1, in sera of the surviving knockout mice, and the reductions were sustained over several months (Fig. 6B). B-1b cells have been proposed to be the primary source of T cell-independent antibody production and long-term protection against *S. pneumoniae* (33, 34). Consistent with this proposition and with our previous data obtained from PC-KLH-immunized DN Bright transgenic mice (39, 48), *Bright* knockout mice exhibited reduced IgM responses to primary immunization with intact *S. pneumoniae* serotype RSA32 cell wall-associated PC (Fig. 6C, left panel).

Functional defects in $Bright^{-/-}$ immune responses are B cell intrinsic. Conventional knockout of *Bright* results in deficiencies in all cell types, compromising conclusions we might draw on intrinsic B cell function. Thus, we generated double-knockout *Bright* ES cell lines (see Materials and Methods) and transferred them into $Rag2^{-/-}$ 129Sv mice by blastocyst complementation (8). Chimeras generated by injection of *Bright* null ES cells had relatively normal numbers and percentages of T cells in thymus and spleen but generally had lower levels of splenic B cells than those resulting from the relatively normal reconstitution achieved by wild-type and *Bright* heterozygous ES cells (Table). 1

As with the conventional knockout mice, $Bright^{-/-}/Rag2^{-/-}$ chimeras exhibited significantly reduced IgM responses to RSA32 cell wall-associated PC (Fig. 6C, lower panel). Mature S107

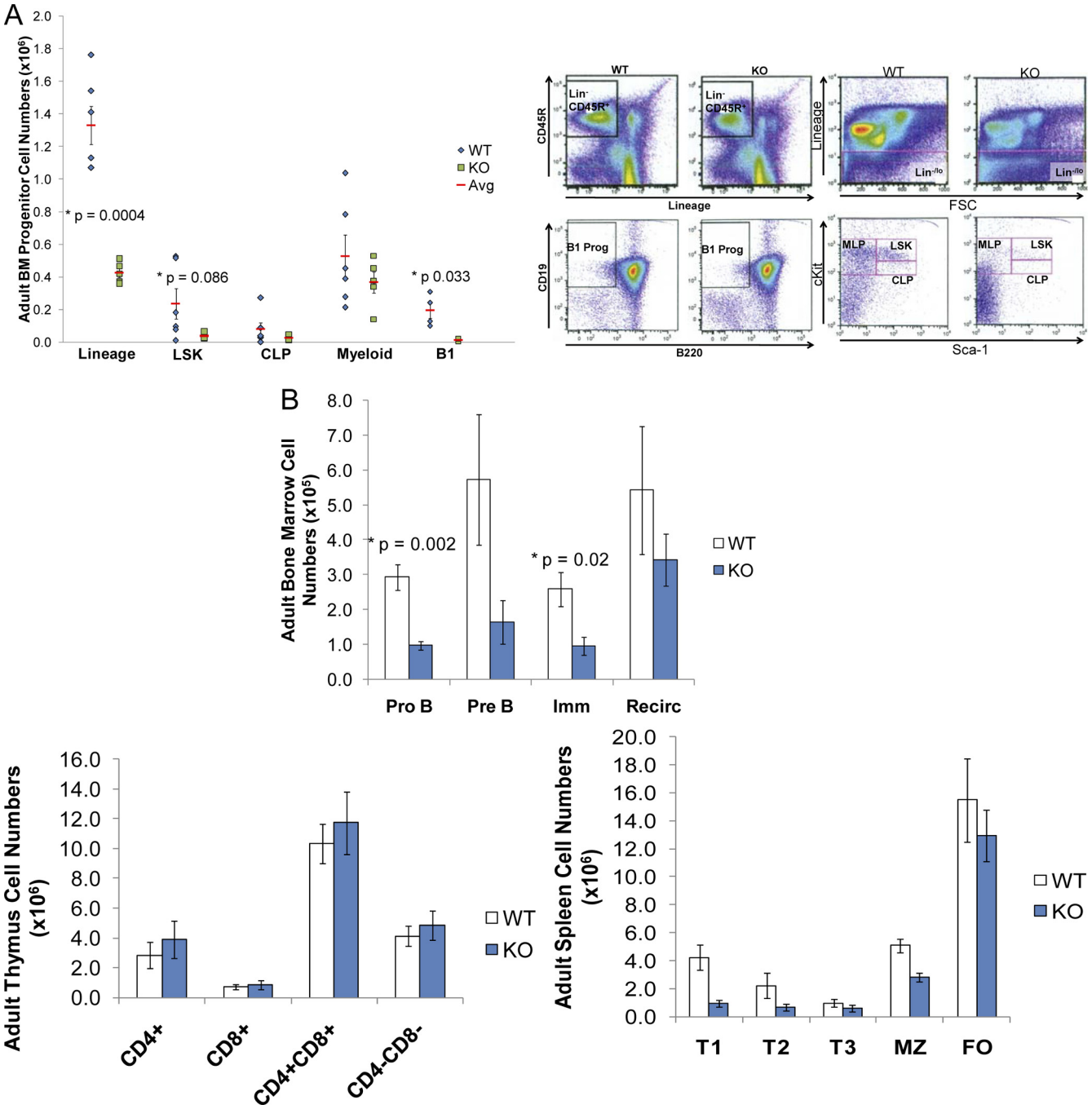

FIG. 5. HSC progenitors and B lineage differentiation are impaired in rare *Bright*$^{-/-}$ mice that survive to adulthood. (A) Total numbers and frequencies of bone marrow (BM) HSC progenitors are reduced in knockout mice. Each symbol represents data obtained from an individual animal (left panel). Representative flow cytometry results show gating of lineage-negative cell subpopulations (upper right panels) used to define the specific progenitor populations shown (lower right panels). B1 Prog, B1 cell progenitor. (B) *Bright* knockouts generate reduced numbers of B lineage cells in bone marrow (upper panel) and spleen (lower right) without affecting T cell lineages in the thymus (lower left). Data were obtained from 10 knockout (KO) and 8 littermate controls (WT). Gating of subpopulations was performed exactly as described in references 40 and 50. Means, standard error bars, and *P* values are shown.

V_H1-Cμ heavy-chain transcripts that encode dominant (T15) anti-IgM responses to PC were downregulated, whereas those corresponding to natural IgM responses encoded by the 7183, J558, and Af303 V_H families were not (Fig. 6C, right panel). These results are consistent with our observations that Bright directly transactivates T15 IgH transcription by binding to DNA consensus motifs within the V_H1 promoter (18, 25, 30, 43, 44, 55, 57, 58).

Bright deficiency results in reduced IgG1 T-dependent responses. Antiprotein responses are typically elicited from FO B cells. Even though the numbers and global proliferation of

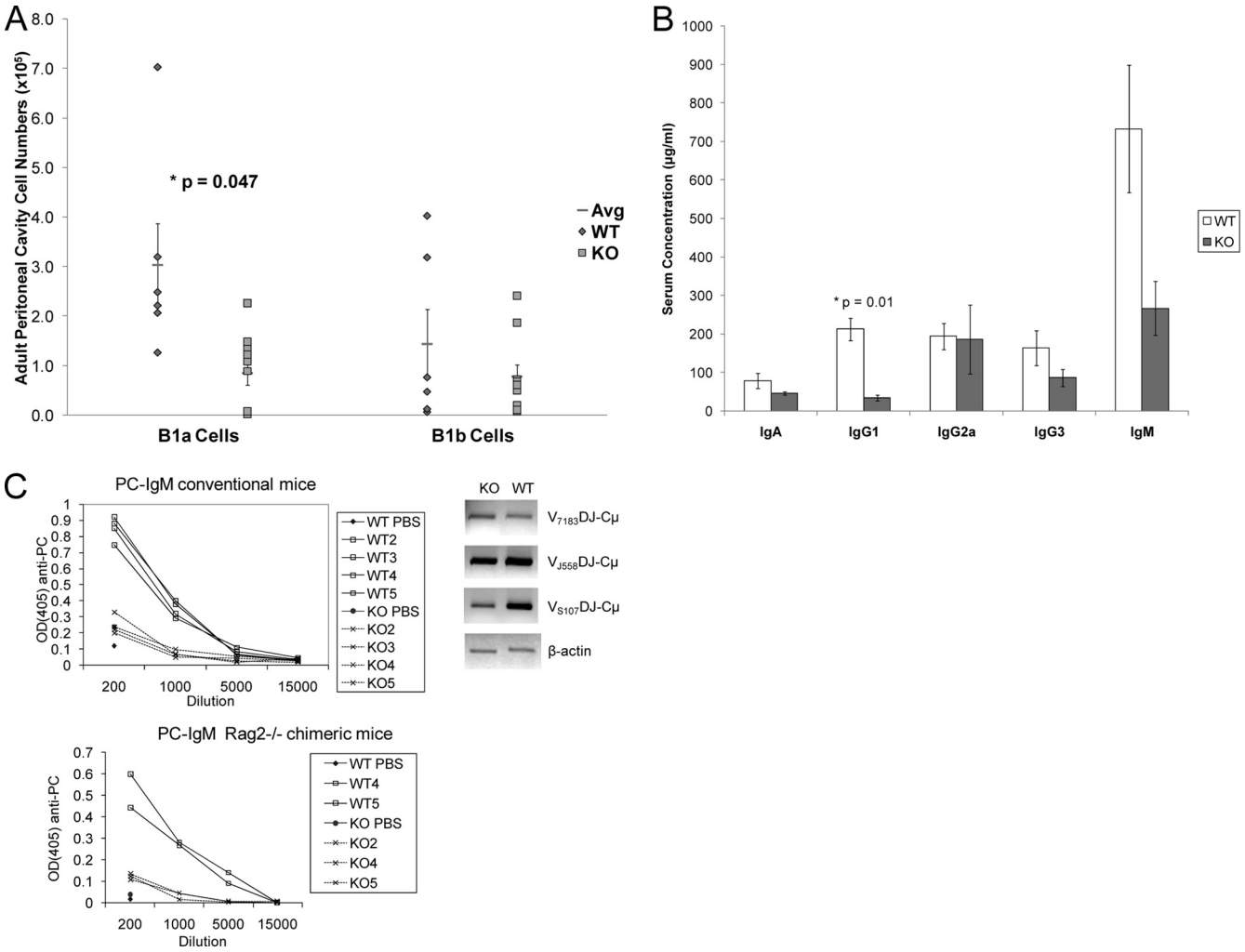

FIG. 6. B-1 cell numbers, natural antibodies, and T-independent responses are compromised in *Bright* knockout mice. (A) *Bright*$^{-/-}$ mice are deficient in mature B-1a (CD19^{+} B220^{+} CD5^{+}) and B-1b (CD19^{+} B220^{+} CD5^{-}) cells in their peritoneal cavities. Each symbol represents an individual mouse. Flow cytometry was performed exactly as described in reference 40. All data are from 6 to 7 mice aged 3 to 6 months; standard error bars and *P* values are shown. (B) *Bright*$^{-/-}$ mice have reduced levels of serum antibodies. Sera were collected from knockout mice and age-matched controls, and isotype levels were measured by ELISA. (C) *Bright*$^{-/-}$ mice exhibit reduced T-independent PC-IgM responses. Groups of 5 *Bright*$^{+/+}$ (WT) or *Bright*$^{-/-}$ (KO) conventional (top left panel) or *Rag2*$^{-/-}$ chimeric (lower left panel) mice were immunized with $\sim 1 \times 10^{8}$ intact *S. pneumoniae* serotype RSA32 cell wall particles, a natural immunogen for PC responses. Sera from these mice were collected 7 days after immunization, and anti-IgM levels were measured by ELISA. Expression of S107 V_H1-Cμ heavy-chain transcripts that encode dominant (T15) anti-IgM PC responses (but not expression of transcripts corresponding to natural IgM responses encoded by the J558 and 7183 V_H families) is reduced following RSA32 immunization. RNA was extracted from spleens of the *Bright*$^{-/-}$/*Rag2*$^{-/-}$ and Bright$^{+/+}$/Rag2$^{-/-}$ immunized mice, and RT-PCR was performed as described in Materials and Methods (right panel).

FO B cells were only modestly reduced in *Bright* null mice (Fig. 5B and data not shown), a defect in the immediate BCR signaling pathway was observed (Fig. 7A). This finding suggested potential functional consequences in antiprotein responses, which are typically elicited from FO B cells. Unexpectedly, however, a defect was observed only for IgG1. T-dependent (TNP-KLH) responses of the *Bright*$^{-/-}$/*Rag2*$^{-/-}$ chimeras (Fig. 7B) as well as of conventional Bright null mice and *Bright*$^{-/-}$ bone marrow-reconstituted C57BL/6 recipients (data not shown) were normal with the exception of significantly reduced secretion of IgG1. These results were consistent with the reduced natural IgG1 sera levels (Fig. 6B). In line with the *in vivo* results, FO B cells purified from spleens of *Bright*$^{-/-}$/*Rag2*$^{-/-}$ chimeras (Fig. 7C, left panel) or from conventional *Bright*$^{-/-}$ mice (data not shown) secreted significantly less IgG1 than controls when stimulated with anti-CD40^{+} IL-4 or LPS. Induction of IgG1 class switching, as measured by the expression of $I_{\gamma 1}$, was reduced 2- to 3-fold in *Bright*$^{-/-}$/*Rag2*$^{-/-}$ chimeras (Fig. 7D, left panel) and even more strongly in the conventional knockout mice (Fig. 7D, right panel), whereas I region-initiated germ line transcription of other isotypes was unperturbed. This provides an explanation for the selective decrease in the frequency of IgG1-switched B cells in the absence of global proliferative changes (data not shown) and suggests that Bright plays a more critical role in the production of IgG1 than in that of other IgG isotypes.

TABLE 1. Comparison of lymphocyte reconstitution in chimeric mice[a]

Genotype	No. (%) of cells of indicated type in the spleen ($\times 10^{-7}$)		No. (%) of SP + DP cells in the thymus ($\times 10^{-7}$)
	B cells	T cells	
Bright$^{+/+}$	5.1 (59)	2.2 (22)	13.4 (97)
Bright$^{+/+}$	4.2 (54)	2.8 (26)	12.5 (98)
Bright$^{+/+}$	4.1 (55)	1.9 (29)	13.1 (98)
Rag2$^{-/-}$	0 (0)	0 (0)	0 (0)
Rag2$^{-/-}$ *Bright*$^{+/+}$	7.5 (65)	3.2 (23)	11.9 (96)
Rag2$^{-/-}$ *Bright*$^{+/+}$	3.5 (38)	1.7 (24)	13.0 (93)
Rag2$^{-/-}$ *Bright*$^{+/-}$	3.1 (41)	2.0 (26)	5.9 (96)
Rag2$^{-/-}$ *Bright*$^{+/-}$	4.3 (53)	0.9 (15)	8.2 (88)
Rag2$^{-/-}$ *Bright*$^{-/-}$	1.9 (32)	1.6 (28)	9.9 (94)
Rag2$^{-/-}$ *Bright*$^{-/-}$	3.7 (29)	2.1 (24)	10.7 (97)
Rag2$^{-/-}$ *Bright*$^{-/-}$	2.8 (40)	1.8 (20)	8.2 (86)

[a] Total numbers were determined by counting with a hemocytometer from single cell suspensions of the indicated organs. Percentages were determined by flow cytometry as B220$^+$ IgM$^+$ for B cells, CD4$^+$ or CD8$^+$ for single positive (SP) T cells, and CD4$^+$ CD8$^+$ for double positive (DP) T cells.

DISCUSSION

Over 20 transcription factors representing a diverse range of DNA binding families have been implicated in hematopoiesis (15, 41). Nearly all of them are associated with hematopoietic malignancy (41). Bright was first described as a B cell-restricted, positive regulator of immunoglobulin gene transcription. Its overexpression in mice, via a B lineage-specific (CD19) promoter-driven transgene, results in enhanced IgM expression and intrinsic B cell autoimmunity but not in cancer. However, Bright ectopic overexpression converts MEFs to tumors in nude mice by bypassing natural or RasV12-induced cellular senescence to promote cellular proliferation via activation of the Rb/E2F1 pathway (42). Bright overexpression, in the absence of locus translocation, correlates with the worst prognosis for patients with the most aggressive form of AID-DLBCL (38). There is no consistent evidence linking *Bright* with chromosomal translocation or somatic mutation, such as that observed for *PU.1* and *C/EBP*α in myeloid malignancies or for *Pax5*, *E2a*, and *EBF* in B-lymphoid malignancies (36). More likely, Bright overexpression leads to lesions in more broadly utilized signaling pathways (e.g., Ras, Rb/E2F1) that regulate hematopoietic lineage decisions. While its oncogenic mechanism remains to be determined, Bright/Arid3a is the first of the 13-member ARID family that fits this unique profile of the major hematopoietic transcription factors.

HSC appear to form normally in *Bright*$^{-/-}$ yolk sacs, but their differentiation into mature erythrocytes is markedly reduced in fetal livers. This results in embryonic death coincident with the shift from primitive to definitive hematopoiesis and the timing of normal Bright expression in fetal liver. Additional work will be required to secure this conclusion, as the contribution of each hematopoietic site (such as the yolk sac and fetal liver) to circulating fetal blood in the fetus or adult has been challenged by recent studies in mice and zebrafish (37, 47). Global *Bright* knockout did not perturb hemoglobin switching, vascularization, or gross organogenesis outside the fetal liver, suggesting a relatively selective role for Bright in HSC expansion and/or differentiation.

It is widely accepted that HSCs of the fetal liver circulate to the adult bone marrow as the source of adult hematopoiesis (28). Accordingly, rare *Bright*$^{-/-}$ survivors show parallel deficiencies in LSK and reduced numbers of common myeloid progenitors (CMP) and CLP in their bone marrow. HSCs residual in fetal liver and bone marrow differ in several properties. Consequently, not all hematopoietic transcription factors regulate both stages. For example, *Sox17* is critical for the generation of fetal, but not bone marrow-derived, HSCs (24). Differential properties include intrinsic programs regulating growth and multilineage differentiation potential, as well as extrinsic differences in engraftment niches required to support these programs (5). Normal fetal liver HSCs are rapidly cycling (15). That overexpression of Bright can activate E2F1 and cell cycle entry in mouse embryonic fibroblasts (42) provides a plausible pathway deregulated by Bright deficiency in this compartment. However, bone marrow HSCs are largely quiescent (15), making it harder to reconcile an analogous role for Bright in sustaining adult hematopoiesis. This implies that as for the principle hematopoietic regulators studied to date (41), Bright function is highly context dependent.

Transcription factors essential for HSC formation and/or self-renewal (e.g., MLL, Runx1, SCL/tal1) often function later within differentiation of separate blood lineages (41). Conversely, factors initially discovered as lineage-restricted regulators (e.g., *PU.1*, *Gfi-1*, *C/EBP*α) were later found to perform essential roles in HSC differentiation (41). Bright is similarly deployed as an intrinsic and specific regulator of the adult B lineage, as T cell and erythroid development (at least at the level of resolution employed in this study) were unaffected in Bright null mice. This finding is consistent with the stringently controlled manner of Bright expression, i.e., present in the earliest identifiable HSC progenitors, downregulated in early pro-B cells and the majority of mature quiescent B cells, and upregulated in pre-B, conventional immature/transitional stages, activated B lymphocytes, and B-1 peripheral compartments (47, 48, 58, 59). *Bright* KO results in B lineage blocking at all post-CLP adult stages, with the exception of the resting FO B cell population and the circulating B cell compartment (which is derived primarily from FO). This can be reconciled by the fact that Bright is normally downregulated in these long-lived compartments (39, 48), which, in addition, are particularly sensitive to homeostatic replenishment even after significant reduction of progenitors following hematopoietic transcription factor knockout (35, 41).

Contrary to a potential compensatory role, *Bdp*$^{-/-}$ embryos died earlier with distinctly different phenotypes. *Bdp* knockouts were developmentally delayed and exhibited aberrant pharyngeal arch development. Bdp expression during this phase of embryogenesis was limited to nascent mesoderm and the neural crest, most prominently within neural crest cells of branchial arches and the neural tube. This is consistent with previous studies that suggested a role for Bdp in craniofacial development and neuroblastoma (27, 52). Thus, it remains unclear why a small percentage of *Bright* null embryos circumvent lethality.

Bright-deficient B cells are intrinsically impaired in mounting primary anti-PC responses. This is due, at least in part, to blocked B-1 development and a selective defect in transcription of the rearranged heavy-chain gene (S107 V_H1) that chiefly encodes PC reactivity (18, 25, 30, 43, 44, 55, 56, 57). For

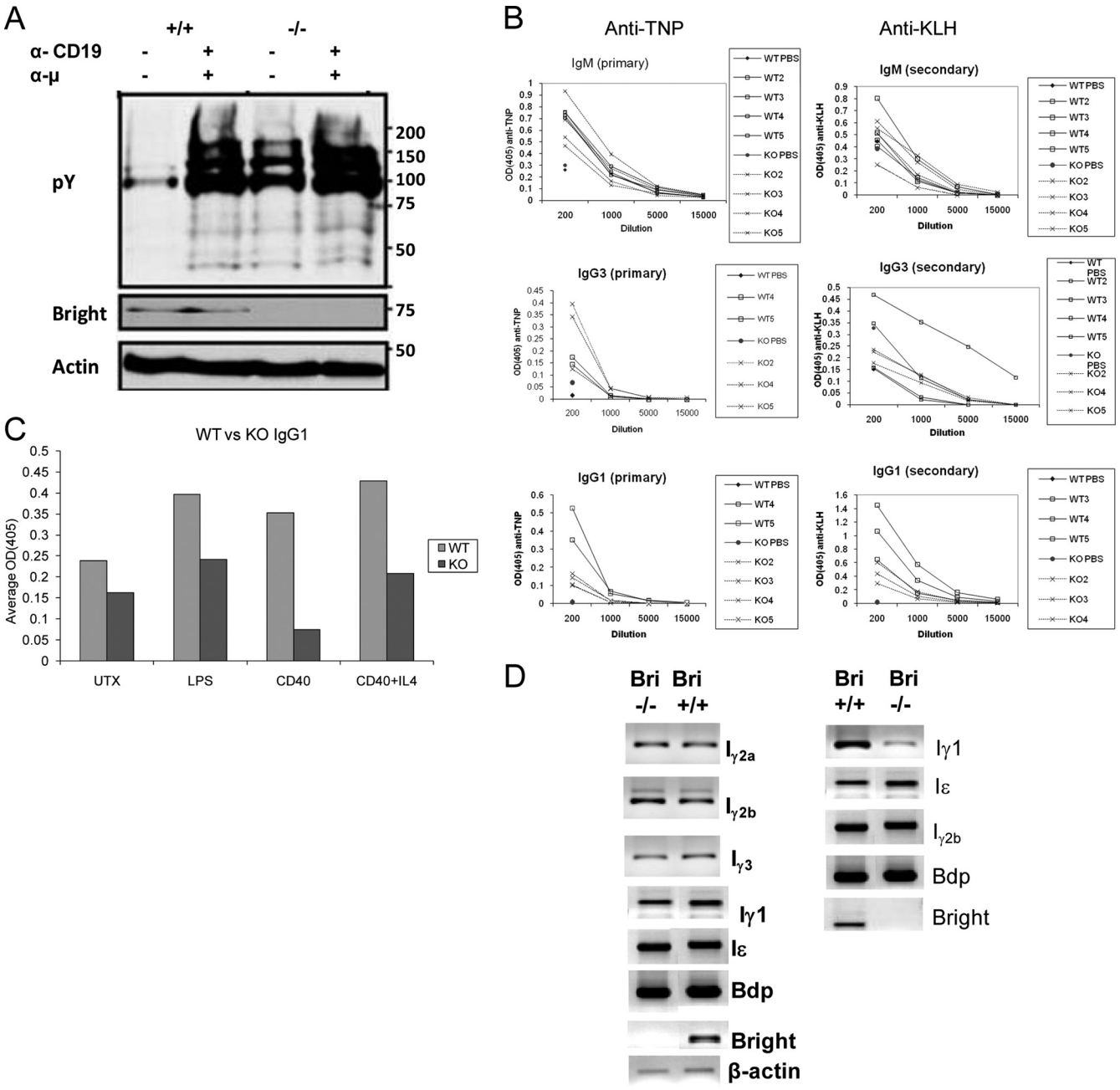

FIG. 7. Selective and intrinsic loss of T-dependent immune function in *Bright*$^{-/-}$ mice. (A) Bright-deficient FO B cells show enhanced proximal signaling prior to and following BCR ligation. Purified FO B cells from wild-type and *Bright*$^{-/-}$ mice (~1 × 10^6/ml) were stimulated with 50 μg of anti-IgM (α-μ) plus 50 μg of anti-CD19 (α-CD19) for 5 min. Western blotting was carried out with antiphosphotyrosine antibody as described previously (48). (B) Reconstituted *Rag2*$^{-/-}$/*Bright*$^{-/-}$ mice are impaired in IgG1 primary and secondary responses to a protein antigen (TNP-KLH). Groups of 5 *Bright*$^{+/+}$ (WT) or *Bright*$^{-/-}$ (KO) mice were primed with 50 μg KLH in adjuvant, and 4 weeks later, they were immunized with TNP-KLH. Sera from these mice were collected 7 days after immunization. Anti-TNP and anti-KLH serum Ig levels were measured by isotype-specific ELISA. Average preimmune serum levels (1:200 serum dilution) are depicted by the solid diamonds and circles. Optical density at 405 nm (OD_{405}) data are shown for each individual mouse from which blood was successfully obtained. (C) Bright deficiency impairs *in vitro* induction of IgG1 secretion but not induction of class switch recombination. Purified splenic FO B cells from *Bright*$^{+/+}$/*Rag2*$^{-/-}$ (WT) and *Bright*$^{-/-}$/*Rag2*$^{-/-}$ (KO) chimeras were left untreated (UTX) or were stimulated at 6 × 10^5/well *in vitro* for 3 days under the conditions indicated (LPS, 20 μg/ml; anti-CD40, 20 μg/ml; and IL-4, 50 ng/ml). Isotype-specific ELISA was carried out as for panel B. Shown are the average values for 5 mice within each group. (D) Bright-deficient follicular B cells are impaired in induction of heavy-chain-γ1 germ line transcripts. FO B cells isolated from splenocytes of *Bright*$^{-/-}$/*Rag2*$^{-/-}$ (left) or *Bright*$^{-/-}$ (right) mice and their wild-type littermate controls were stimulated *in vitro* for 3 days with anti-CD40 (20 μg/ml) and IL-4 (50 ng/ml). Primers and conditions for semiquantitative RT-PCR analyses are described in Materials and Methods.

maximum transcriptional activation function, Bright must interact with Btk, an essential transducer of BCR signaling, and TFII-I, a direct phosphorylation substrate of Btk (43, 44). Btk is required for both B-1 generation and normal PC responses (11) and acts principally at the checkpoints (pre-B1 and T1) most compromised in both *Bright* KO and DN mice (13).

These defects were previously observed, albeit less dramatically, in Bright DN transgenic mice (39). The differences in penetrance most likely derive from incomplete DN inhibition, particularly in HSC and early B lineage progenitors, where the transgenic B cell-specific promoter (CD19) is either inactive or significantly weakened (19). Concentration-dependent effects in lineage choice and differentiation are well documented (12, 29, 45). Alternatively, Bright can act outside the nucleus, independently of DNA binding, to dampen signal transduction via association with BCR and Btk in plasma membrane lipid rafts (48). We suspect that this function, which remains unperturbed in DN transgenic B cells, may contribute to the proximal signaling hyperactivity we observed in the knockout FO B cells. Potentially relevant in this regard, Btk can modulate EpoR/c-kit signaling to drive expansion of erythroid progenitors (53). On the other hand, we have recently observed that B cells from both Bright knockout and DN transgenic mice are developmentally plastic (1). Further experiments will be required to more accurately define the mechanism by which Bright deficiency leads to these phenotypic changes.

Bright-deficient FO B cells, while only modestly reduced in number, are intrinsically defective in generating T-dependent IgG1 responses. Selective reduction in IgG1 can be explained, at least in part, by selective reduction in IL-4$^+$ anti-CD40 stimulation of γ1 germ line transcription, a prerequisite for class switch recombination (CSR) and the production of mature γ1 mRNA (50). While these results implicate Bright in CSR, the mechanism underlying the observed γ1 specificity is unclear. One possibility is that a gene critical to the process is a direct target deregulated by the knockout of Bright. For example, particular NF-κB transcription factors can promote germ line transcription in general (16) or specifically promote γ1 germ line transcription (3) by binding to specific I regions and/or to the 3′ enhancer, a CSR control region located downstream of the IgH locus (50). Alternatively, Bright might function at the level of the intergenic switch (S) region sequences that facilitate the recombination step of CSR. Elegant knockout experiments by Bhattacharya et al. (4) suggest that the switch to γ1 is facilitated in a physiological setting by an as-yet-unidentified IL-4-induced factor that has specific DNA binding for Sγ1. Bright expression is induced by IL-4$^+$ anti-CD40 (48, 49, 58, 59), and the Sγ1 region is particularly rich in MARs (10), the motif to which Bright binds (18, 60).

Hematopoietic transcription factors operate through diverse mechanisms, but association with chromatin modification proteins is a consistent theme (15, 41). Examples include Ikaros-NuRD in the T lineage (26), EKLF-Brg1 in the erythroid lineage (7), and Gfi-LSD1 in the myeloid lineage control (46). Bright binding to MARs within the IgH enhancer promotes chromatin accessibility (22, 30). Other ARID family members directly remodel chromatin (60). The challenge of future experiments is to identify relevant non-IgH transcriptional targets of Bright and to determine whether Bright acts via chromatin-associated factors to promote HSC differentiation and post-CLP B lineage programming.

ACKNOWLEDGMENTS

We thank S. Ferrell, Chhaya Das, Deborah Surman, and Maya Ghosh for technical assistance.

Support was provided by NIH 044215 (C.F.W.), NIH CA31534 (P.W.T.), CPRIT (P.W.T. and M.P.), and the Marie Betzer Morrow Endowment (P.W.T.).

We have no financial conflict of interest.

REFERENCES

1. **An, G., et al.** 2010. Loss of Bright/ARID3a function promotes developmental plasticity. Stem Cells **28:**1560–1567.
2. **Angelin-Duclos, C., and K. Calame.** 1998. Evidence that immunoglobulin V_H-DJ recombination does not require germ line transcription of the recombining variable gene segment. Mol. Cell. Biol. **18:**6253–6264.
3. **Bhattacharya, D., D. U. Lee, and W. C. Sha.** 2002. Regulation of Ig class switch recombination by NF-κB: retroviral expression of RelB in activated B cells inhibits switching to IgG1, but not to IgE. Int. Immunol. **14:**983–991.
4. **Bhattacharya, P., R. Wuerffel, and A. L. Kenter.** 2010. Switch region identity plays an important role in Ig class switch recombination. J. Immunol. **184:** 6242–6248.
5. **Bowie, M. B., et al.** 2007. Identification of a new intrinsically timed developmental checkpoint that reprograms key hematopoietic stem cell properties. Proc. Natl. Acad. Sci. U. S. A. **104:**5878–5882.
6. **Briles, D. E., et al.** 1981. Antiphosphocholine antibodies found in normal mouse serum are protective against intravenous infection with type 3 *Streptococcus pneumoniae*. J. Exp. Med. **153:**694–705.
7. **Bultman, S. J., T. C. Gebuhr, and T. Magnuson.** 2005. A Brg1 mutation that uncouples ATPase activity from chromatin remodeling reveals an essential role for SWI/SNF-related complexes in β-globin expression and erythroid development. Genes Dev. **19:**2849–2861.
8. **Chen, J., R. Lansford, V. Stewart, F. Young, and F. W. Alt.** 1993. RAG-2-deficient blastocyst complementation: an assay of gene function in lymphocyte development. Proc. Natl. Acad. Sci. U. S. A. **90:**4528–4532.
9. **Chen, X., R. S. Welner, and P. W. Kincade.** 2009. A possible contribution of retinoids to regulation of fetal B lymphopoiesis. Eur. J. Immunol. **39:**2515–2524.
10. **Cockerill, P. N.** 1990. Nuclear matrix attachment occurs in several regions of the IgH locus. Nucleic Acids Res. **18:**2643–2648.
11. **Contreras, C. M., et al.** 2007. Btk regulates multiple stages in the development and survival of B-1 cells. Mol. Immunol. **44:**2719–2728.
12. **DeKoter, R. P., and H. Singh.** 2000. Regulation of B lymphocyte and macrophage development by graded expression of PU.1. Science **288:**1439–1441.
13. **Desiderio, S.** 1997. Role of Btk in B cell development and signaling. Curr. Opin. Immunol. **9:**534–540.
14. **Fuxa, M., et al.** 2004. Pax5 induces V-to-DJ rearrangements and locus contraction of the immunoglobulin heavy-chain gene. Genes Dev. **18:**411–422.
15. **Garrison, B. S., and D. J. Rossi.** 2010. Controlling stem cell fate one substrate at a time. Nat. Immunol. **11:**193–194.
16. **Gerondakis, S., and U. Siebenlist.** 2010. Roles of the NF-κB pathway in lymphocyte development and function. Cold Spring Harb. Perspect. Biol. **2:**a000182.
17. **Griffin, C. T., J. Brennan, and T. Magnuson.** 2008. The chromatin-remodeling enzyme BRG1 plays an essential role in primitive erythropoiesis and vascular development. Development **135:**493–500.
18. **Herrscher, R. F., et al.** 1995. The immunoglobulin heavy-chain matrix-associating regions are bound by Bright: a B cell-specific trans-activator that describes a new DNA-binding protein family. Genes Dev. **9:**3067–3082.
19. **Hobeika, E., et al.** 2006. Testing gene function early in the B cell lineage in mb1-cre mice. Proc. Natl. Acad. Sci. U. S. A. **103:**13789–13794.
20. **Hogan, B., R. Beddington, F. Costantini, and E. Lacey.** 1994. Recovery, culture, and transfer of embryos and germ cells, p. 130. *In* Manipulating the mouse: a laboratory manual, 2nd ed. Cold Spring Harbor Laboratory Press, Cold Spring Harbor, NY.
21. **Huang, Y. J., et al.** 2008. Targeting the human cancer pathway protein interaction network by structural genomics. Mol. Cell. Proteomics **7:**2048–2060.
22. **Kaplan, M. H., R. T. Zong, R. F. Herrscher, R. H. Scheuermann, and P. W. Tucker.** 2001. Transcriptional activation by a matrix associating region-binding protein: contextual requirements for the function of Bright. J. Biol. Chem. **276:**21325–21330.
23. **Kearney, J. F., R. Barletta, Z. S. Quan, and J. Quintáns.** 1981. Monoclonal vs. heterogeneous anti-H-8 antibodies in the analysis of the anti-phosphorylcholine response in BALB/c mice. Eur. J. Immunol. **11:**877–883.
24. **Kim, D., L. Probst, C. Das, and P. W. Tucker.** 2007. REKLES is an ARID3-restricted multifunctional domain. J. Biol. Chem. **282:**15768–15777.

25. **Kim, D., and P. W. Tucker.** 2006. A regulated nucleocytoplasmic shuttle contributes to Bright's function as a transcriptional activator of immunoglobulin genes. Mol. Cell. Biol. **26:**2187–2201.
26. **Kim, J., et al.** 1999. Ikaros DNA-binding proteins direct formation of chromatin remodeling complexes in lymphocytes. Immunity **10:**345–355.
27. **Kobayashi, K., T. Era, A. Takebe, L. M. Jakt, and S. Nishikawa.** 2006. ARID3B induces malignant transformation of mouse embryonic fibroblasts and is strongly associated with malignant neuroblastoma. Cancer Res. **66:** 8331–8336.
28. **Laird, D. J., U. H. von Andrian, and A. J. Wagers.** 2008. Stem cell trafficking in tissue development, growth, and disease. Cell **132:**612–630.
29. **Laslo, P., et al.** 2006. Multilineage transcriptional priming and determination of alternate hematopoietic cell fates. Cell **126:**755–766.
30. **Lin, D., et al.** 2007. Bright/ARID3A contributes to chromatin accessibility of the immunoglobulin heavy chain enhancer. Mol. Cancer **6:**23.
31. **Liu, G., et al.** 2010. Solution NMR structure of the ARID domain of human AT-rich interactive domain-containing protein 3A: a human cancer protein interaction network target. Proteins **78:**2170–2175.
32. **Manis, J. P., et al.** 1998. Class switching in B cells lacking 3′ immunoglobulin heavy chain enhancers. J. Exp. Med. **188:**1421–1431.
33. **Martin, F., and J. F. Kearney.** 2001. B1 cells: similarities and differences with other B cell subsets. Curr. Opin. Immunol. **13:**195–201.
34. **Martin, F., A. M. Oliver, and J. F. Kearney.** 2001. Marginal zone and B1 B cells unite in the early response against T-independent blood-borne particulate antigens. Immunity **14:**617–629.
35. **Motoda, L., et al.** 2007. Runx1 protects hematopoietic stem/progenitor cells from oncogenic insult. Stem Cells **25:**2976–2986.
36. **Mullighan, C. G., et al.** 2007. Pediatric acute myeloid leukemia with NPM1 mutations is characterized by a gene expression profile with dysregulated HOX gene expression distinct from MLL-rearranged leukemias. Leukemia **21:**2000–2009.
37. **Murry, C. E., and G. Keller.** 2008. Differentiation of embryonic stem cells to clinically relevant populations: lessons from embryonic development. Cell **132:**661–680.
38. **Ngo, V. N., et al.** 2006. A loss-of-function RNA interference screen for molecular targets in cancer. Nature **441:**106–110.
39. **Nixon, J. C., et al.** 2008. Transgenic mice expressing dominant-negative Bright exhibit defects in B1 B cells. J. Immunol. **181:**6913–6922.
40. **Numata, S., P. P. Claudio, C. Dean, A. Giordano, and C. M. Croce.** 1999. Bdp, a new member of a family of DNA-binding proteins, associates with the retinoblastoma gene product. Cancer Res. **59:**3741–3747.
41. **Orkin, S. H., and L. I. Zon.** 2008. Hematopoiesis: an evolving paradigm for stem cell biology. Cell **132:**631–644.
42. **Peeper, D., et al.** 2002. A functional screen identifies hDRIL1 as an oncogene that rescues RAS-induced senescence. Nat. Cell Biol. **4:**148–153.
43. **Rajaiya, J., M. Hatfield, J. C. Nixon, D. J. Rawlings, and C. F. Webb.** 2005. Bruton's tyrosine kinase regulates immunoglobulin promoter activation in association with the transcription factor Bright. Mol. Cell. Biol. **25:**2073–2084.
44. **Rajaiya, J., et al.** 2006. Induction of immunoglobulin heavy-chain transcription through the transcription factor Bright requires TFII-I. Mol. Cell. Biol. **26:**4758–4768.
45. **Roeder, I., and I. Glauche.** 2006. Towards an understanding of lineage specification in hematopoietic stem cells: a mathematical model for the interaction of transcription factors GATA-1 and PU.1. J. Theor. Biol. **241:** 852–865.
46. **Saleque, S., J. Kim, H. M. Rooke, and S. H. Orkin.** 2007. Epigenetic regulation of hematopoietic differentiation by Gfi-1 and Gfi-1b is mediated by the cofactors CoREST and LSD1. Mol. Cell **27:**562–572.
47. **Samokhvalov, I. M., N. I. Samokhvalova, and S. Nishikawa.** 2007. Cell tracing shows the contribution of the yolk sac to adult haematopoiesis. Nature **446:**1056–1061.
48. **Schmidt, C., et al.** 2009. Signalling of the BCR is regulated by a lipid rafts-localised transcription factor, Bright. EMBO J. **28:**711–724.
49. **Shankar, M., et al.** 2007. Anti-nuclear antibody production and autoimmunity in transgenic mice that overexpress the transcription factor Bright. J. Immunol. **178:**2996–3006.
50. **Stavnezer, J., J. E. J. Guikema, and C. E. Schrader.** 2008. Mechanism and regulation of class switch recombination. Annu. Rev. Immunol. **26:**261–292.
51. **Stryke, D., et al.** 2003. BayGenomics: a resource of insertional mutations in mouse embryonic stem cells. Nucleic Acids Res. **31:**278–281.
52. **Takebe, A., et al.** 2006. Microarray analysis of PDGFRα^+ populations in ES cell differentiation culture identifies genes involved in differentiation of mesoderm and mesenchyme including ARID3b that is essential for development of embryonic mesenchymal cells. Dev. Biol. **293:**25–37.
53. **von Lindern, M., U. Schmidt, and H. Beug.** 2004. Control of erythropoiesis by erythropoietin and stem cell factor: a novel role for Bruton's tyrosine kinase. Cell Cycle **3:**876–879.
54. **Wang, B., et al.** 2004. Foxp1 regulates cardiac outflow tract, endocardial cushion morphogenesis and myocyte proliferation and maturation. Development **131:**4477–4487.
55. **Webb, C., C. Das, S. Eaton, K. Calame, and P. Tucker.** 1991. Novel protein-DNA interactions associated with increased immunoglobulin transcription in response to antigen plus interleukin-5. Mol. Cell. Biol. **11:**5197–5205.
56. **Webb, C., et al.** 1999. Differential regulation of immunoglobulin gene transcription via nuclear matrix-associated regions. Cold Spring Harb. Symp. Quant. Biol. **64:**109–118.
57. **Webb, C. F., C. Das, K. L. Eneff, and P. W. Tucker.** 1991. Identification of a matrix-associated region 5′ of an immunoglobulin heavy chain variable region gene. Mol. Cell. Biol. **11:**5206–5211.
58. **Webb, C. F., et al.** 1998. Expression of Bright at two distinct stages of B lymphocyte development. J. Immunol. **160:**4747–4754.
59. **Webb, C. F., et al.** 2000. The transcription factor Bright associates with Bruton's tyrosine kinase, the defective protein in immunodeficiency disease. J. Immunol. **165:**6956–6965.
60. **Wilsker, D., et al.** 2005. Nomenclature of the ARID family of DNA-binding proteins. Genomics **86:**242–251.